JCTC Journal of Chemical Theory and Computation

ARTICLE

pubs.acs.org/JCTC

Tuned Range-Separated Time-Dependent Density Functional Theory Applied to Optical Rotation

Monika Srebro[†,‡] and Jochen Autschbach*[,†]

[†]Department of Chemistry, University at Buffalo, State University of New York, Buffalo, New York 14260-3000, United States

[‡]Department of Theoretical Chemistry, Faculty of Chemistry, Jagiellonian University, R. Ingardena 3, 30-060 Krakow, Poland

Supporting Information

ABSTRACT: For range-separated hybrid density functionals, the consequences of using system-specific range-separation parameters (γ) in calculations of optical rotations (ORs) are investigated. Computed ORs at three wavelengths are reported for methyloxirane, norbornenone, β-pinene, [6]helicene, [7]helicene, and two derivatives of [6]helicene. The γ parameters are adjusted such that Kohn−Sham density functional calculations satisfy the condition $-\varepsilon^{\mathrm{HOMO}}(N) = \mathrm{IP}$. For β-pinene, the behavior of the energy as a function of fractional total charge is also tested. For the test set of molecules, comparisons of ORs with available coupled-cluster and experimental data indicate that the γ "tuning" leads to improved results for β-pinene and the helicenes and does not do too much harm in other cases.

1. INTRODUCTION

Quantum-chemical methods based on Kohn−Sham density functional theory (DFT) and its time-dependent extension (TDDFT)[1−4] have proven to be valuable tools in a broad variety of scientific fields including chemistry, biochemistry, physics, material sciences, spectroscopy, and catalysis.[5−16] Despite their widespread popularity and great success in determination of properties for a wide variety of systems, several problems have been established in practical calculations that can be traced to the spurious electron self-repulsion present in commonly used approximations.[17−23] In particular, many conventional generalized gradient approximations (GGA) and hybrid GGA exchange-correlation (XC) functionals fail in a qualitative and quantitative description of diffuse valence and Rydberg states as well as charge-transfer excitations due to incorrect asymptotic behavior and deficient long-range exchange. These issues affect computed molecular response properties, such as polarizabilities and optical rotations, to varying degrees ranging from insignificant to severe. Apart from early methods for treating self-interaction and recovering asymptotic behavior,[24−27] a conceptually straightforward approach that has been proposed is the use of range-separated (long-range corrected, LC; Coulomb-attenuated method, CAM) functionals.[28−31] As has been shown, such functionals offer remedies for origin problems.[32−40]

In range-separated hybrid DFT the electron repulsion entering the exchange term of the Kohn−Sham energy functional is split into long-range and short-range parts by using for example the standard error function as in the Coulomb-attenuated method (CAM) of Yanai et al.[30]

$$\frac{1}{r_{12}} = \frac{\alpha + \beta\,\mathrm{erf}(\gamma r_{12})}{r_{12}} + \frac{1 - [\alpha + \beta\,\mathrm{erf}(\gamma r_{12})]}{r_{12}} \qquad (1)$$

Here, α and β are dimensionless parameters satisfying the relations $0 \le \alpha + \beta \le 1$, $0 \le \alpha \le 1$, and $0 \le \beta \le 1$. They quantify the importance of the HF/DFT contribution in the short-range/long-range region. At r_{12} close to 0, the fraction of HF exchange is α, and its DFT counterpart is $1 - \alpha$. As r_{12} gets larger, the exchange is increasingly described by the HF expression rather than through DFT, approaching a fraction of $\alpha + \beta$ with r_{12} approaching ∞. The range-separation parameter γ (in a_0^{-1} units) determines the balance of DFT to HF exchange at intermediate r_{12}, governing how rapidly the long-range limit is attained. A smaller/larger value results in slower/faster replacement of DFT exchange by its HF counterpart with an increase in interelectronic distances. For $\beta = 0$, the fraction of HF exchange is α over the whole range, which corresponds to conventional (global) hybrids. With $\alpha = 0$ and $\beta = 1$, the original LC approach of Iikura et al.[28] is reproduced, in which short-range exchange is represented purely by a local potential derived from the LDA or the GGA approximations. Fully long-range corrected functionals require $\alpha + \beta = 1$. The popular functional CAM-B3LYP does not fully switch to 100% HF but gives only 65% of exact exchange at large interelectronic distances with $\alpha = 0.19$ and $\beta = 0.46$ parameters determined through a fit to the atomization energies of a standard set of molecules.[30]

As benchmark studies have shown, the performance of long-range corrected functionals is sensitive to the parametrization.[34,35,41−44] In particular, a strong dependence of calculated ground- and excited-state properties on the range-separation parameter has been revealed. In most implementations, γ is adjusted in order to minimize average errors in equilibrium distances, atomization energies, barrier heights, ionization energies, and/or other ground-state properties of a test set of molecules and treated as a universal constant for subsequent computations. Typical γ ranges from 0.30 to 0.50 a_0^{-1} with recommended values of 0.33,[29] 0.40,[28,33] 0.47,[45] and 0.50, depending on the functional.[32,37] The optimal value differs,

Received: October 27, 2011
Published: November 30, 2011

however, for the properties of interest as well as for the specific systems being studied.[41,43] A practical, physically motivated method for determining system-specific range-separation parameters has been recently suggested by Livshits and Baer in ref 37, utilized in refs 46−48. The suggested tuning procedure is based on the requirement that in exact Kohn−Sham theory, the negative of the energy of the highest occupied molecular orbital (HOMO) in the N electron system is equal to the ionization potential (IP) calculated as a ground-state energy difference

$$-\varepsilon^{\mathrm{HOMO}}(N) = \mathrm{IP} = E_{\mathrm{gs}}(N-1) - E_{\mathrm{gs}}(N) \quad (2)$$

Accordingly, γ can be adjusted to a given molecular system by minimizing

$$\Delta E(\gamma) = \varepsilon^{\mathrm{HOMO}}(N;\gamma) + [E_{\mathrm{gs}}(N-1;\gamma) - E_{\mathrm{gs}}(N;\gamma)] \quad (3)$$

Above, the assumption is made that the same γ is appropriate for both the N and the $N-1$ electron systems. The tuned LC-(TD)DFT approach has been already successfully applied to several problems considered until recently as too difficult for DFT[23,46−52] with the γ value varying substantially with the system under consideration. For example, for simple inorganic molecules, the optimal γ range is from 0.3 a_0^{-1} for Li_2; through 0.5 a_0^{-1} for CH_2O and NH_3 to 0.7 a_0^{-1} for HF, O_2, and F_2; and 0.8 a_0^{-1} for P_2.[37,51] In all of these studies, the long-range corrected Baer, Neuhauser, and Livshits (BNL) functional[31,37] was utilized. Herein, we adopt the γ tuning procedure in its original, simplest form[37] for other popular range-separated functionals and apply it in optical rotation calculations that were found to be notoriously challenging for TDDFT.

An alternative, related way of improving a functional in a system-specific way is to enforce the correct behavior of the energy E as a function of the electron number N,[36,53] which is also sometimes referred to as the straight line theorem:[54] The energy of an atom or molecule as a function of N changes linearly for N varying between two integers. The slope of $E(N)$ changes discontinuously as N passes through integers (derivative discontinuity). For instance, as N passes through the electron number of a neutral atom, the slope of $E(N)$ changes from −IP (ionization potential) to −EA (electron affinity). As an example, Vydrov et al. used the straight line criterion to assess the quality of the LC-ωPBE functional in comparison with standard GGAs and hybrid GGAs;[36] see also the Supporting Information (SI) accompanying this article (Figure S4). Similarly, Cohen et al.[53] and Tsuneda et al.[55] examined the energy for fractional charges with other range-separated functionals.

Optical rotation (OR) has been established as a valuable tool in the determination of the absolute configuration (AC) of chiral molecules. The protocol employs a comparison of a measured OR for a candidate stereoisomer with theoretical predictions for a known absolute configuration.[56−62] To effectively utilize such a method, however, a robust and reliable approach to predicting optical rotations from first principles need to be applied. On the basis of studies by Stephens et al.,[63] the B3LYP hybrid functional with the aug-cc-pVDZ basis set based on geometry optimizations with the 6-31G(d) basis is often considered the standard protocol for OR calculations. The robustness and limitations of this level of theory have been explored in many benchmarks.[60,64,65] Expected improvements for a description of Rydberg and charge-transfer states offered by range-separated functionals as compared to standard (global) hybrids and GGAs prompted us recently to pursue a benchmark study (OR45) in order to examine the performance of such functionals in OR calculations for a diverse set of molecules ranging from small organic systems to organometallic complexes.[66] The intimate relation between the OR and the excitation spectrum implies that better performance of LC functionals should be observed. Our results, however, showed that, on average, the two range-separated functionals (LC-PBE0 and CAM-B3LYP) do not outperform their global hybrid counterparts for the OR45 test set.[66] This finding does not necessarily indicate a failure of the range-separation concept itself but may rather imply the need of ab initio-motivated molecule-specific reparametrization of the currently used LC functionals. The fact that a partial or full long-range correction was established to be beneficial in selected cases seems to corroborate this conclusion.[66] For instance, for norbornenone, the OR calculated with LC-PBE0/aug-cc-pVDZ was found to be close to coupled-cluster (CC) reference data and very different from the B3LYP result. The correct sign of the OR of β-pinene, a notoriously difficult case for computations, was also reproduced at this level of theory with the corresponding magnitude close to a gas-phase value interpolated from experimental data. Accordingly, taking into account the promising performance of tuned range-separated XC functionals in many types of computations,[49] and for Rydberg and charge-transfer excitations in particular, in the present study we examine such an approach to calculations of optical rotation for selected molecules of the OR45 benchmark differing in size and type of chromophores (Figure 1). The list of functionals studied herein includes LC-PBE and LC-BLYP, as well as the hybrids, LC-PBE0 and CAM-B3LYP (in its default and a modified parametrization). For literature references and parametrization details, see section 2. For the test systems, diffuse valence and Rydberg states (heterocycles, bicycles) and 'charge-transfer-character' excitations (helicenes), as postulated for linear and nonlinear polycyclic aromatic hydrocarbons,[48,67] can be expected to contribute significantly to the OR, and thus a tuned TDDFT approach, ensuring their accurate description, should be especially advantageous.

In the following, we first provide additional technical details regarding the computations (section 2). Optical rotations obtained with tuned and nontuned functionals are reported along with experimental and CC reference data in section 3. A detailed analysis of the performance of fully long-range corrected functionals is provided, followed by a discussion of the behavior of

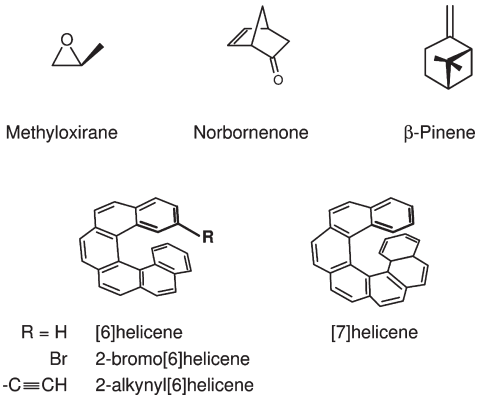

Figure 1. Molecular structures and absolute configurations of the systems studied herein.

Coulomb-attenuated hybrids. A test of various XC functionals for a system with fractional electron numbers is also presented in this section. Finally, a brief summary and an outlook is given in section 4. The γ tuning appears to help with the ORs of β-pinene and the helicenes. In the other cases, when considering variations among the highest level calculations available in the literature, the results do not significantly deteriorate when a tuned γ parameter is used. On the basis of these findings, the tuning procedure can be cautiously recommended for applications to electronic optical activity.

2. COMPUTATIONAL DETAILS

Calculations were carried out for the molecules shown in Figure 1 in the absolute configurations as indicated, with the exception of 2-alkynyl[6]helicene. For this system, computations for the optical antipode were performed, and the corresponding optical rotations are reported here with the opposite sign of the ones calculated. The γ tuning procedure was performed for methyloxirane, norbornenone, β-pinene, and two helical systems, 2-alkynyl[6]helicene and [7]helicene. OR computations include also two other helicenes, [6]helicene and 2-bromo[6]helicene. Optimized structures for all of the systems studied here were taken from ref 66. Symmetry was not explicitly utilized in the calculations.

The computations were performed with a locally modified developer's version of the Northwest Computational Chemistry (NWChem) package[68,69] using the augmented correlation-consistent Dunning basis set, aug-cc-pVDZ.[70,71] Functionals examined in this work include long-range corrected variants of PBE[72,73] and PBE0,[74,75] labeled here as LC-PBE ($\gamma = 0.30\ a_0^{-1}$, $\alpha = 0, \beta = 1$) and LC-PBE0[43] ($\gamma = 0.30\ a_0^{-1}$, $\alpha = 0.25, \beta = 0.75$), and two parametrizations of the Coulomb-attenuated version of B3LYP:[76−79] CAM-B3LYP in its original parametrization with $\alpha + \beta = 0.65$ ($\gamma = 0.33, \alpha = 0.19, \beta = 0.46$)[30] and a fully long-range corrected modification, LC-B3LYP, with $\alpha = 0.19$ and $\beta = 0.81$, $\alpha + \beta = 1.0$. Some computations utilized the LC variant of BLYP,[76,77] LC-BLYP ($\gamma = 0.33\ a_0^{-1}$, $\alpha = 0$, $\beta = 1$). In parentheses, the default parametrization of each functional as recommended in the NWChem manual is given. For comparison, OR calculations were carried out with B3LYP and Hartree−Fock (HF) as well. The ab initio system-specific determination of range-separation parameter γ was performed via minimizing the function given by eq 3. In single-point ground-state calculations of neutral and corresponding cation radical systems, an energy convergence threshold of 10^{-10} au was applied for all molecules with the exception of 2-alkynyl[6]helicene, for which 10^{-7} au was used.

For tests of the energy as a function of noninteger electron numbers, fractional orbital occupations and fractional total electron numbers were implemented in a developer's version of NWChem. Details will be provided elsewhere. The code was verified by a comparison of $E(N)$ for the carbon atom calculated with Hartree−Fock and various density functionals with reference data from the literature.[36] See the SI (Figure S4) for a plot of $E(N)$ for carbon.

Optical rotation (OR) calculations were carried out with a recently developed TDDFT linear response module ("AOResponse") implemented in NWChem[80,81] and utilized the GIAO dipole length gauge to ensure origin invariance of isotropic ORs. The optical rotation parameters were computed at the sodium line wavelength $\lambda = 589.3$ nm ($\omega = 0.07732$ au), as well as $\lambda = 355$ ($\omega = 0.128$ au) and 633 nm (0.0720 au) to compare with available OR data from gas-phase cavity ring-down polarimetry (CRDP) measurements[82−84] and coupled-cluster data from the literature. The "xfine" integration grid was employed in numerical integrations of the XC potential and the XC response kernel. Convergence criteria were set to 10^{-10} au and 10^{-6} au for the SCF and coupled perturbed Kohn−Sham (CPKS) procedure, respectively. A default parameter of 10^{-5} au was used in the computations to remove linearly dependent basis function combinations.

Optical rotations are discussed herein in terms of molar rotations (MRs), $[\phi]$. The calculated molecular OR parameter β can be converted to the observable specific rotation (excluding local field corrections or concentrations effects) via

$$[\alpha] = 7200\ \text{deg}\ \frac{\omega^2 N_A}{c^2 M}\,\beta(\omega)$$

and further to molar rotation by

$$[\phi] = [\alpha]\,\frac{M}{100}$$

In the equations above, the "circular" frequency of the perturbing field ω is in units of s^{-1}; $\beta(\omega)$ is in units of cm^4. Further, N_A, c, and M are Avogadro's number, the speed of light (in cm s^{-1}), and the molecular weight (in g mol^{-1}), respectively. The units of $[\alpha]$ and $[\phi]$ are deg/[dm (g/cm^{-3})] and deg cm^2 $dmol^{-1}$, respectively. To put our results in perspective, where available we have included both experimental as well as coupled-cluster results reported in the literature, converting specific rotations given in each case to molar rotations. For brevity, range-separation parameter units of a_0^{-1} and molar rotation units of deg cm^2 $dmol^{-1}$ are frequently dropped from here on.

3. RESULTS AND DISCUSSION

3.1. Fully Long-Range Corrected Functionals Applied to OR Calculations. The calculated ΔE as a function of γ according to eq 3 for methyloxirane, norbornenone, and β-pinene using the aug-cc-pVDZ basis set and the fully long-range corrected functionals LC-PBE, LC-PBE0, and LC-B3LYP are graphically presented in Figure 2. A γ range from 0.1 to0.5 a_0^{-1} was considered in each case. For norbornenone, some calculations with LC-PBE0 and LC-B3LYP with γ close to 0.5 failed to reach SCF convergence for the radical cation, and the corresponding data points in Figure 2 have been omitted. The numerical values of $\Delta E(\gamma)$ are collected in Tables S1−S3 of the Supporting Information (SI).

$\Delta E(\gamma)$ changes considerably within the γ ranges shown in Figure 2. In each case, however, a particular value of γ can be found below 0.4 a_0^{-1}, for which the condition $\Delta E(\gamma) = 0$ is satisfied. In the following, the values of the range-separation parameter rendering a very small (close to 0) $\Delta E(\gamma)$ and corresponding to the (ionization from the HOMO) minimum are denoted as the optimal values γ^*.

The system-specific range-separation parameters differ from the global ones (0.30 for LC-PBE and LC-PBE0, 0.33 for LC-B3LYP) to varying degrees, with deviations ranging from 0.02 to 0.11. For the LC hybrids, the γ^* values are always decreased compared to the universal γ parameters, which implies that the contribution of exact exchange at short-range in such cases is smaller than assumed on the basis of the universal γ. The change is especially pronounced for β-pinene (0.11 difference). In the case of LC-PBE, the γ tuning has mixed directions, with γ^* decreased with respect to the universal value for β-pinene

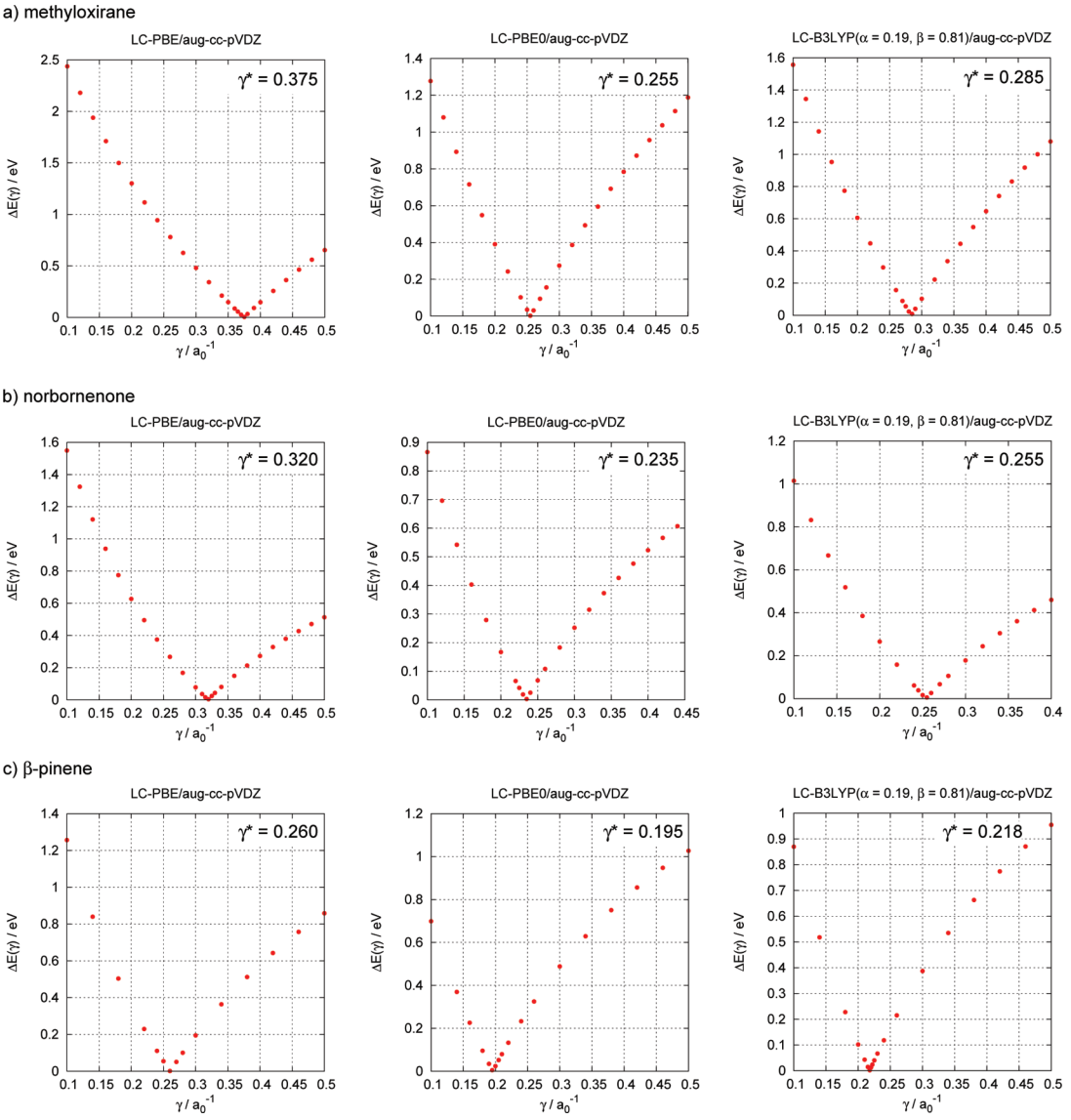

Figure 2. ΔE of eq 3 as a function of the range-separation parameter γ. Calculations with LC-PBE, LC-PBE0, and LC-B3LYP, for methyloxirane (top row), norbornenone (center row), and β-pinene (bottom row). The numerical γ^* values listed in the panels correspond to $\Delta E \approx 0$.

(by 0.04) but increased for norbornenone (by 0.02) and methyloxirane (by 0.08). In all cases, the smallest γ^* is determined for β-pinene and the largest for methyloxirane.

The corresponding molar rotations (MRs) at 355, 589, and 633 nm calculated using individually tuned γ^* and universal (empirically fitted) γ values are listed in Table 1 for LC-PBE and LC-PBE0 and in Table 2 for LC-B3LYP. For each molecule, experimental data and optical rotations obtained from approximate correlated wave function theories (CCSD and CC2) are provided as well.

There are many possible factors determining a reliable and accurate theoretical prediction of optical rotation within a given level of quantum-chemical methodology, among which the intrinsic quality of the electronic structure, conformational averaging, vibrational corrections, and solvent effects are of the highest importance. Since we have not included vibrational corrections and solvent effects in the calculations, it is more reasonable to assess the performance of the DFT methods by comparison with gas-phase single-point results from the best available wave function based ab initio methods, for instance, coupled-cluster theory, rather than experimental solution data. As reference data, we have chosen the recent CCSD results of ORs by Mach and Crawford[85] calculated with a modified velocity gauge (MVG)[86] and aug-cc-pVDZ basis set used in our study. In the case of norbornenone and β-pinene, due to the high computational cost, higher order CC data are not available in the literature. Comparisons with the results calculated with the double aug-cc-pVDZ basis set imply rather little basis set dependence of their ORs at the CCSD level. The situation is very different for methyloxirane. Noticeable differences between the CCSD values obtained with various basis sets as well as between optical rotations calculated with successive models of coupled-cluster theory of potentially increasing accuracy indicate that the chosen CCSD/aug-cc-pVDZ reference data are not converged in terms of basis sets and electron correlation effects.[85,87,88] Accordingly, in the discussion, we have referred to CC3 data available in the literature as well. Some comparisons with gas-phase cavity ring-down polarimetry measurements are also made.

Table 1. Molar Rotations for Methyloxirane, Norbornenone, and β-Pinene Calculated with aug-cc-pVDZ and the LC-PBE and LC-PBE0 Functionals

			LC-PBE			LC-PBE0		
	$[\phi]^{exptl.a}$	$[\phi]^{CCSD}/[\phi]^{CC2b}$	$[\phi]\gamma = 0.30^{c}$ ($[\phi]\gamma = 0.47^{d}$)	γ^{*e}	$[\phi]\gamma^{*}$	$[\phi]\gamma = 0.30^{c}$	γ^{*e}	$[\phi]\gamma^{*}$
			355 nm					
methyloxirane	4.35	−32.8/−43.3	−18.03 (−26.15)	0.375	−23.89	−21.60	0.255	−19.84
norbornenone		−4213.1/−6699.1	−8959 (−5598)	0.320	−8297	−6345	0.235	−7474
β-pinene	92.2	115.4/276.4	86.21 (0.952)	0.260	128.2	45.32	0.195	123.2
			589.3 nm					
methyloxirane	−10.9	−17.5/−26.5	−12.05 (−11.90)	0.375	−12.25	−11.22	0.255	−11.23
norbornenone	−1239	−605.5/−880.6	−1044 (−815.2)	0.320	−1002	−892.9	0.235	−983.6
β-pinene	−31.5	1.0/34.7	−4.751 (−18.84)	0.260	1.725	−11.06	0.195	1.751
			633 nm					
methyloxirane	−4.87	−15.4/−23.3	−10.67 (−10.42)	0.375	−10.77	−9.874	0.255	−9.908
norbornenone		−498.3/−721.4	−854.4 (−672.4)	0.320	−821.2	−735.2	0.235	−807.8
β-pinene	−6.35	−1.0/27.2	−5.587 (−17.12)	0.260	−0.310	−10.72	0.195	−0.234

[a] 589.3 nm, solution data from refs 89−91; 355 and 633 nm, gas-phase data from ref 84. [b] CCSD and CC2/aug-cc-pVDZ/MVG data from ref 85. [c] Universal γ value as implemented in NWChem. [d] Universal γ value as implemented in Gaussian. [e] Optimal γ value as determined in this work.

Table 2. Molar Rotations for Methyloxirane, Norbornenone, and β-Pinene Calculated with aug-cc-pVDZ and the LC-B3LYP and CAM-B3LYP Functionals

			LC-B3LYP			CAM-B3LYP	
	$[\phi]^{exptl.a}$	$[\phi]^{CCSD}/[\phi]^{CC2b}$	$[\phi]\gamma = 0.33^{c}$	γ^{*d}	$[\phi]\gamma^{*}$	$[\phi]\gamma = 0.33^{c}$	$[\phi]\gamma^{*}$
			355 nm				
methyloxirane	4.35	−32.8/−43.3	−16.82	0.285	−13.54	−13.13	−9.940
norbornenone	−5315.1	−4213.1/−6699.1	−6089	0.255	−7418	−7754	−8937
β-pinene	92.2	115.4/276.4	70.55	0.218	173.7	161.3	240.3
			589.3 nm				
methyloxirane	−10.9	−17.5/−26.5	−10.61	0.285	−10.40	−10.83	−10.55
norbornenone	−1239	−605.5/−880.6	−860.8	0.255	−891.5	−999.5	−1080
β-pinene	−31.5	1.0/34.7	−7.150	0.218	9.040	8.400	19.86
			633 nm				
methyloxirane	−4.87	−15.4/−23.3	−9.398	0.285	−9.257	−9.646	−9.440
norbornenone	−520.2	−498.3/−721.4	−708.9	0.255	−791.4	−820.0	−883.5
β-pinene	−6.35	−1.0/27.2	−7.543	0.218	5.681	5.247	14.56

[a] 589.3 nm, solution data from refs 89−91; 355 and 633 nm, gas-phase data from ref 84. [b] CCSD and CC2/aug-cc-pVDZ/MVG data from ref 85. [c] Universal γ value as implemented in NWChem. [d] Optimal γ value as determined in this work.

In the following discussion, unsigned relative deviations of computed data with respect to reference values (experimental or other theoretical data), i.e. $\Delta^{r} = |[\phi]_D^{calcd} - [\phi]_D^{ref}|/|[\phi]_D^{ref}|$, in percent, will be utilized.

Methyloxirane. Consider first the data obtained for a small rigid three-ring member of the test set, methyloxirane, which is among the most extensively studied systems for optical rotation. Recently, Mach and Crawford[85] reported CCSD/aug-cc-pVDZ/MVG MRs

of −32.8, −17.5, and −15.4 deg cm^2 dmol^{-1} for 355, 589.3, and 633 nm, respectively. These results deviate noticeably from the experimental gas-phase data, especially at 355 nm, for which CCSD gives the opposite sign. HF/aug-cc-pVDZ/GIAO results determined by us (355, −14.58; 589.3, −7.534; 633 nm, −6.640) agree with the coupled-cluster data in terms of sign, although the significant drop in the magnitude can be observed due to the lack of electron correlation effects. The B3LYP functional appears to perform somewhat better than CCSD in delivering optical rotations closer to experimental results: 0.811, −9.950, and −9.036 deg cm^2 dmol^{-1}, respectively. The problem of discrepancies between computed CC and gas-phase experimental data for methyloxirane is now well understood and attributed to zero-point vibrational corrections (ZPVCs).[88,92−94] The seemingly good performance of B3LYP at 355 nm was shown to be due to a significant underestimation of the lowest (Rydberg) excitation energy leading to a fortuitous positive shift in the MR toward the experimental result.[87] Accordingly, taking into account the importance of Rydberg states for this molecule, it is expected that the correct asymptotic behavior of range-separated XC functionals may be especially beneficial here, improving the agreement between DFT and CC results.

According to the data collected in Tables 1 and 2, the three LC functionals in their standard parametrization perform reasonably well for methyloxirane when compared to the coupled-cluster data. The DFT values are located somewhere between Hartree−Fock and CC. The relative deviations from the CCSD data are similar at 589.3 and 633 nm and range from 31 to 39% with the following ordering of functionals in terms of delivering the best agreement with the reference data: LC-PBE > LC-PBE0 > LC-B3LYP. As can be seen, the better agreement is obtained with vanishing short-range HF exchange contributions. At 355 nm both PBE-based functionals still outperform the fully long-range corrected version of CAM-B3LYP, LC-B3LYP. However, the best agreement with CC is now obtained for LC-PBE0. The corresponding relative deviations Δ^r are LC-PBE = 45, LC-PBE0 = 34, and LC-B3LYP = 49%. For the two longer wavelengths, using the LC-PBE functional with a γ value of 0.47 a_0^{-1} as implemented in the Gaussian package[95] increases only slightly the relative deviations from CC, by 0.9−1.7%. However, at 355 nm, a significant decrease is observed, by 25%. Accordingly, it appears that at this wavelength the MR is especially sensitive to the functional parametrization and the short-range exact exchange contribution.

Using the first-principles tuned range-separation parameter γ^* changes the results to an insignificant degree at 589.3 and 633 nm. The γ tuning noticeably influences the optical rotations at 355 nm, as should be expected from the discussion in the previous paragraph. An increase from 0.30 to the tuned value of 0.38 a_0^{-1} for LC-PBE leads to a MR closer to the coupled-cluster data with Δ^r decreased to 27%. This is in line with the aforementioned improved performance of LC-PBE with γ = 0.47. In the case of the tuned LC hybrid functionals, the tuning produces an increase of the relative deviation to CC data by 5.4% for LC-PBE0 and by 10% for LC-B3LYP.

Assuming that zero-point vibrational corrections (ZPVC) calculated at one level of theory are to a good degree transferable to another level of OR calculations, we have used CCSD ZPVCs from ref 93, 20.05 and 3.74 deg cm^2 dmol^{-1} for 355 and 633 nm, respectively, in conjunction with our equilibrium ORs discussed above. Resulting MRs ranging from −6.105 to 6.513 at 355 nm and from −7.029 to −5.516 at 633 nm are closer to experimental values than vibrationally corrected coupled-cluster data of −12.8 and −11.7. Keeping in mind the incomplete convergence of the CCSD/aug-cc-pVDZ OR reference data in terms of basis sets and electron correlation effects, to get additional insight into the performance of the tuned TDDFT approach for this molecule, we have recalculated MRs at the LR-PBE level with the aug-cc-pVDZ, aug-cc-pVTZ,[70,71] and d-aug-cc-pVDZ[70,71,96] basis sets for C, O, and H, respectively, and compare them with available corresponding CC3 results of −13.5 and −10.3 deg cm^2 dmol^{-1} at 355 and 589.3 nm.[88] Our MRs are −16.71 and −11.30/−22.63 and −11.55 for the nontuned/optimal γ parameter. There is better agreement between standard parametrizations of LC DFT and these CC3 data than what is discussed above for the CCSD/aug-cc-pVDZ reference values. For tuned LC-PBE, at 589.3 nm, we find Δ^r = 24% with respect to CC3, but at 355 nm, Δ^r = 68%. Therefore, the assessment is inconclusive. Taking into account a strong dependence of optical rotation of methyloxirane on the CC level and the basis set quality, as well as structural parameters,[87] further studies appear to be in order to reliably assess the methyloxirane results for the tuned γ parameters.

Norbornenone. Norbornenone has a very large optical rotation at 589.3 nm, which was attributed to electronic coupling between the two π systems, C═C and C═O, present in this molecule.[97,98] CCSD has been shown to strongly underestimate the experimental solution-phase MR.[65,85,99] Likewise, we have recently shown that range-separated hybrids give MRs for norbornenone that are in some cases significantly below the solution-phase experimental values.[66] Nonhybrid DFT significantly overestimates the optical rotation.[66,100,101] Vibrational corrections were shown to be relatively minor when compared to the equilibrium optical rotation.[102]

We approach the discussion with the assumption that the available CCSD data are representative of gas-phase measurements. CCSD/aug-cc-pVDZ/MVG MRs of norbornenone calculated recently by Mach and Crawford[85] at 355, 589.3, and 633 nm are −4213, −605.5, and −498.3 deg cm^2 dmol^{-1}, respectively. They are comparable to HF data (GIAO) of −3389, −645.6, and −537.8, which suggests that electron correlation, although not negligible, is not a major influence for the optical rotation of norbornenone. On the other hand, density functionals show a large variation in the calculated MRs, in particular as a function of HF exchange.[66] Thus, the main factor influencing the norbornenone OR is likely the exchange, or lack thereof, in approximate functionals. Since CCSD and HF yield MRs that are much closer to each other than the variations between pure GGAs and global hybrids, for instance, correlation effects offered by DFT are potentially of secondary importance for norbornenone, while exact exchange becomes of paramount relevance (see below for further discussion.)

As Tables 1 and 2 show, the standard NWChem parametrizations of asymptotically corrected LC-PBE, LC-PBE0, and LC-B3LYP functionals lead to MR values ranging from −6089 (45%) to −8959 (113%) at 355 nm, from −860.8 (42%) to −1044 (72%) at 589.3 nm, and from −708.9 (42%) to −854.4 deg cm^2 dmol^{-1} (72%) at 633 nm (relative deviations from CC in parentheses). Although these functionals overestimate the MR magnitude, they yield better agreement with CCSD than the global hybrid B3LYP, which produces MRs of −12370 (193), −1291 (113), and −1051 (111%) at 355, 589.3, and 633 nm, respectively. In terms of agreement with CCSD, the functional performance is LC-B3LYP > LC-PBE0 > LC-PBE. The agreement becomes better as the fraction of the HF exchange in the functional at shorter interelectronic separations, determined by γ as well as

the α parameters, increases. This trend is further confirmed by LC-PBE calculations using the Gaussian value of $\gamma = 0.47$. In this case, the larger γ translates to a larger HF exchange contribution already at shorter interelectronic distances, which may compensate the lack of a fixed global HF contribution in this functional ($\alpha = 0$). The increased γ relative to the default parameters led to a significant decrease of Δ^r, between 37 and 80%, at each wavelength. Accordingly, this parametrization of LC-PBE outperforms both LC hybrids.

The results calculated with the tuned functionals remain in line with our finding that the larger HF contribution at short-range improves the agreement with CCSD. In the case of both range-separated hybrids for which the tuned γ^* is smaller than the default value, the agreement with CCSD somewhat deteriorates. For LC-PBE, γ^* is slightly higher than the default value, and improved agreement with CCSD is obtained. As in the case of methyloxirane, for all functionals, the short wavelength optical rotation is more sensitive to the range-separation parameter value/short-range HF contribution in terms of variations in Δ^r.

Although the optical rotations of norbornenone calculated at both tuned and nontuned LC-TDDFT levels remain significantly different from the CCSD results, it is worth noting that they match very well with results of the CC2 (second-order approximate CCSD) model.[103] This may imply that in terms of reproducing correlation effects the DFT methods considered here are closer in performance to CC2 than to CCSD. Using the optimized range-separation parameter generally leads to somewhat lessened agreement with CC2 for the LC-PBE0 and LC-B3LYP functionals and some improvements for LC-PBE. The sizable differences between CC2 and CCSD, however, also raise questions about the convergence of the wave function results with respect to the level of correlation. Going from HF to CC2 indicates that correlation plays a significant role in the optical rotation of norbornenone. The CCSD data are closer to HF again, reversing the trend from HF to CC2. One might infer from these trends that either CC2 artificially produces correlation effects that are not really present in the molecule or that lower order and higher order correlation effects cancel to a large degree. In the latter case, convergence might be difficult to achieve. When assessing the performance of the density functionals, it is important to keep in mind that, because the HF and CCSD reference data are reasonably close to each other, parameter changes that produce more HF exchange overall at the expense of correlation will give better agreement with the reference data. If there is a hidden role of correlation in the final result, the seemingly better performance obtained from such parameter tweaks might be for the wrong reason. We tentatively attribute the improvements from range-separated LC exchange, compared to pure DFT functionals and global hybrids, to the correct asymptotic behavior of the XC potentials.

During the course of this study, we noticed that the best agreement with CCSD is obtained with the LC-BLYP functional in its parametrization as implemented in the Gaussian package ($\gamma = 0.47$), yielding molar rotations of -5462, -799.1, and -659.1 deg cm^2 dmol^{-1} at 355, 589.3, and 633 nm, respectively (slightly outperforming LC-PBE with the same γ). Tuning leads to $\gamma^* = 0.32$ a_0^{-1}. For the $\Delta E(\gamma)$ graph and the numerical data, see Figure S1 and Table S2 of the SI. The corresponding calculated MRs at 355, 589.3, and 633 nm are -8202, -987.8, and -809.1, thus strongly increased in magnitude as compared to the results with the $\gamma = 0.47$. For comparison, the default NWChem parametrization gives results of -7774, -960.2, and -787.2, which are bracketed by those obtained with higher and lower γ. The decrease in the MR magnitude with an increased HF contribution at shorter range remains in line with the findings for the other functionals.

β-Pinene. β-pinene is among the most problematic cases for OR calculations; most levels of theory fail to reproduce the sign of the experimentally observed optical rotation. Recent CCSD data by Mach and Crawford[85] (355, 115.4; 589.3, 1.0; and 633 nm, -1.0 deg cm^2 dmol^{-1}) agree reasonably well with CRDP measurements of 92.2 and -6.4 at 355 and 633 nm, as well as with an interpolated gas-phase value of -3.8 at 589.3 nm.[65] The large deviation between CCSD and the liquid-state MR at the sodium D line must be attributed to solution-phase experiment versus gas-phase calculation. HF theory strongly underestimates the MR at 355 nm (19.57) and overestimates it at long wavelengths (-16.73 and -15.49 deg cm^2 dmol^{-1}), leading also to the wrong sign at 589.3 nm. B3LYP produces MRs that are too high in magnitude (342.2, 34.76, 26.70) and fails to reproduce the CCSD sign for both of the long wavelengths.

The LC functionals in their default parametrizations perform somewhat better than HF and B3LYP, leading in each case to noticeably decreased relative deviations from the CCSD reference data. Again, an underestimation of the MR at 355 nm is observed, with the relative deviations from CCSD ranging from 25 to 61%. At 589.3 nm, none of the functionals considered here reproduce the sign and magnitude of the CCSD MR. At 633 nm, the signs agree with CCSD but, as in the case of the sodium D line, with a significant overestimation of the absolute value. The relative deviations range from 575 to 1206% and from 459 to 972% for 589.3 and 633 nm, respectively, owing to the small magnitude of the reference value. In terms of delivering the best agreement with the CCSD, the ordering of the functionals is LC-PBE > LC-B3LYP > LC-PBE0. For LC-PBE, using $\gamma = 0.47$ as a default in the Gaussian package leads to a significant deterioration of the calculated MR. Especially at 355 nm, the calculated MR of 0.952 deg cm^2 dmol^{-1} is far from the expected range of values. However, the result is in line with the trend of increasing MR with decreasing γ as detailed in the next paragraph. Overall, most of the TDDFT calculation values produce reasonable agreement with experimental data (generally better than the agreement with CCSD), with Δ^r ranging from 6.5 to 77%.

According to the data listed in Tables 1 and 2, the LC PBE-based (GGA and hybrid) functionals with the optimized range-separation parameter perform very similar in the β-pinene optical rotation calculations. A substantial improvement of the MRs is obtained from the γ tuning, with relative deviations from CCSD of 6.8 to 11 at 355, 72 to 75 at 589.3, and 69 to 77% at 633 nm. In each case, the CCSD OR sign is reproduced. Although the tuned LC-PBE and LC-PBE0 results are closer to the coupled-cluster MRs, they are further away from experimental results. The tuned parametrization of LC-B3LYP gives a deterioration rather than improvement, with the MR sign reproduced only for 355 and 589.3 nm and highly overestimated magnitudes.

Pristine and Substituted Helicenes. Recently, LC functionals have been shown to provide more reliable excitation energies for planar polyaromatic hydrocarbons and their helical isomers than conventionally used (TD)DFT approximations.[48,67,104−106] It has been postulated that the improved performance is linked to a partial charge-transfer character of the $\pi \rightarrow \pi^*$ transitions in extended π chromophores.[48,67] Likewise, it has been found

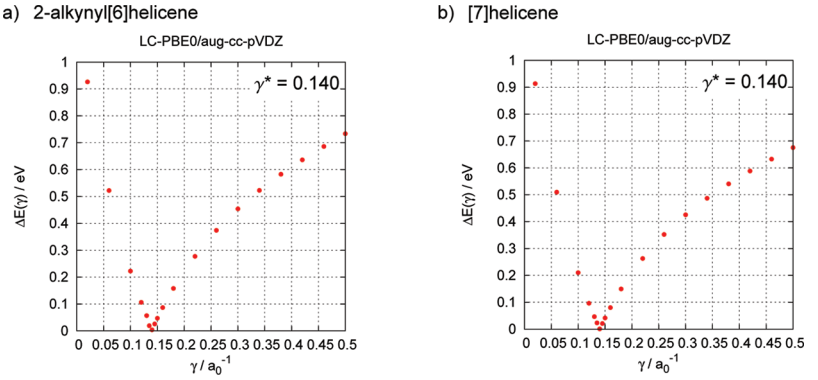

Figure 3. ΔE of eq 3 as a function of the range-separation parameter γ. LC-PBE0 calculations for 2-alkynyl[6]helicene (panel a) and [7]helicene (panel b). The printed γ^* values correspond to $\Delta E \approx 0$.

recently that range-separated hybrid functionals in their standard parametrizations tend to outperform global hybrids in optical rotation calculations of helicenes systems.[66] A counterexample is [7]helicene where a significant underestimation of the MR magnitude with respect to the solution-phase experiment was obtained, in particular for LC-PBE0. Taking into account promising results for excitation energies of oligoacene series and related hydrocarbons obtained with γ-tuned TDDFT,[48] it is therefore interesting to investigate whether system-specific γ parameters lead to improved optical rotations of helicenes and helicene derivatives.

Results of the tuning procedure performed for 2-alkynyl-[6]helicene and [7]helicene with LC-PBE0 are graphically presented in Figure 3. The corresponding numerical data for $\Delta E(\gamma)$ are collected in Table S4 of the SI. The optimal γ parameter determined according to eq 3 is the same, 0.14 a_0^{-1}, for both systems. This value nicely corresponds to results obtained for a series of oligacenes $C_{2+4n}H_{4+2n}$ (n = 1−6) reported recently in refs 47 and 48, for which the tuned γ parameters decrease with system size, from 0.31 for benzene (n = 1) to 0.19 for hexacene (n = 6). Qualitatively, one may relate the decrease in the optimal γ to an increased range of delocalization in the π systems, making it beneficial to have short-range DFT exchange present in the functional at comparatively large interelectronic distances. The optimized range-separation parameter value is significantly decreased compared to the default parameter on the order of 0.3 typically used.

Calculated molar rotations (LC-PBE0/aug-cc-pVDZ) are collected in Table 3 along with solution-phase experimental data. The γ^* value determined for 2-alkynyl[6]helicene and [7]helicene was also applied in calculations of pristine [6]helicene and its bromo-substituted derivative. The following conclusions can be drawn on the basis of the presented data. (*i*) In the case of [7]helicene, using the optimized range-separation parameter in place of 0.30 leads to a significant improvement of the calculated MR toward the solution-phase experiment, with the relative deviation decreasing from 36 to 15%. For 2-alkynyl[6]helicene, in turn, the relative deviation increases from 19 to 56%. (*ii*) Optical rotations for [6]helicene and 2-bromo[6]helicene benefit from the optimized γ value, with a Δ^r of merely 5 and 6%. (*iii*) The dependence of the helicenes OR on structural parameters was previously studied in ref 66. Using geometries optimized with Grimme's dispersion-corrected DFT (specifically: DFT-D3)[111] leads to a deterioration of the calculated optical rotations. Although

Table 3. Molar Rotations (in deg cm^2 dmol^{-1}) for Helicenes and Helicene Derivatives Calculated with LC-PBE0/aug-cc-pVDZ

		$[\phi]^{calcd.}$	
	$[\phi]^{exptl.a}$	γ = 0.30[b]	γ^* = 0.14[c]
2-alkynyl[6]helicene	−11042	−13183	−17245
[7]helicene	−23465	−15108	−19980
		−12048[d]	−15818[d]
			(−15709)[d]
[6]helicene	−11954	−9921.4	−12569
2-bromo[6]helicene	−14500	−11937	−15379

[a] Solution data from refs 107−110. [b] Universal γ value, default parametrization. [c] Optimal γ as determined in this work for 2-alkynyl-[6]helicene and [7]helicene. [d] Molar rotation for structure optimized with DFT-D3; in parentheses: molar rotation obtained with optimal γ of 0.143 a_0^{-1} determined for DFT-D3 geometry.

the tuned LC-PBE0 with γ = 0.14 subsequently improves the result for [7]helicene, the underestimation of the optical rotation with DFT-D3 geometries remains substantial (relative deviation of 33%). The tuning procedure performed for the DFT-D3 structure (Figure S2 and Table S4 of Supporting Information) leaves the optimal range parameter almost unchanged (0.143).

On the basis of computations on large carbon structures,[111,112] the DFT-D structures are expected to significantly better represent the gas-phase helicene geometries. The effect of dispersion corrections on structural parameters of 2-bromo[6]helicene is detailed in the Supporting Information of ref 66. As was shown, dispersion corrections appear to substantially overestimate interactions between the aromatic rings at opposing ends of the helicene moieties when the optimized geometries are compared to the X-ray crystal structure. Accordingly, it seems likely that dispersion interactions are quenched in the crystal environment. The good agreement between nondispersion-corrected DFT and experimental geometries of organometallic helicene complexes[113,114] corroborates this hypothesis. A similar situation is plausible also for the liquid phase, although further work on solvated systems would appear necessary to study these effects in more detail. We tentatively consider the structures optimized without dispersion corrections to be more suitable to reproduce solution-phase ORs. The solvent may also cause direct influences on the optical rotations which are not modeled. The UV−vis spectrum of

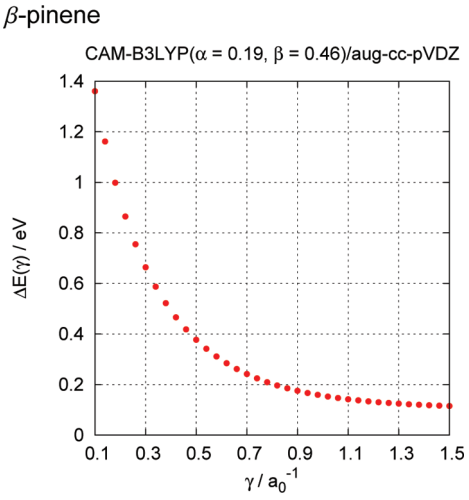

Figure 4. ΔE of eq 3 as a function of the range-separation parameter γ calculated with CAM-B3LYP for β-pinene.

these systems is dominated by valence excitations. It is therefore expected that condensed-phase effects are modest, compared to systems such as methyloxirane and the bicyclic cage structures investigated herein for which excitations involving diffuse orbitals are very important already at comparatively long wavelengths.

3.2. Coulomb-Attenuated Method CAM-B3LYP Applied to OR Calculations. The CAM-B3LYP functional utilizes $\alpha = 0.19$ and $\beta = 0.46$ in its original parametrization, minimizing errors for atomization energies for a test set of molecules.[30] Thus, by switching to only 65% of HF exchange at large interelectronic distances, the CAM-B3LYP XC potential V_{XC} does not afford the correct $-1/r$ behavior asymptotically. The different features of CAM-B3LYP as compared to LC functionals makes it an interesting case in the context of adjusting the range-separation parameter.

Tozer and Handy,[27] going back to arguments put forward by Perdew et al.,[54,115] showed that, for continuum functionals, V_{XC} does not go to zero asymptotically. Rather, $V_{XC}(\infty) = \mathrm{IP} + \varepsilon^{HOMO}$, where both values on the right-hand side correspond to calculations with the same functional. Tozer[21] later showed that the charge-transfer failure of TDDFT, which is corrected by LC functionals, is intimately related to the integer discontinuity in the XC potential, $\Delta = V_{XC}^{+} - V_{XC}^{-}$, which globally shifts the potential by a constant as the electron number for the system passes through an integer. The "+" and "−" indicate here a system with a slight excess and a slight deficiency of a fractional electron. "Pure" LDA and GGA density functionals do not exhibit this discontinuity. Tozer showed that in this case $\varepsilon^{HOMO} \approx -\mathrm{IP} + \Delta/2$.[21] Thus, the situation where $V_{XC}(\infty) = \mathrm{IP} + \varepsilon^{HOMO} \neq 0$ is likely connected to the integer discontinuity problem where $\varepsilon^{HOMO} + \mathrm{IP} \approx \Delta/2 \neq 0$. A pure DFT component in a functional that is not fully long-range corrected to enforce $V_{XC}(\infty) = 0$ may therefore prevent the condition of eq 3 to be fulfilled, except for the extreme case where $\gamma \rightarrow \infty$, which would completely suppress the short-range DFT exchange.

Figure 4 shows results for eq 3 for β-pinene calculated with CAM-B3LYP for different values of γ. Similar plots for methyloxirane and norbornenone can be found in Figure S3 of the SI. The corresponding numerical values $\Delta E(\gamma)$ are listed in Tables S1−S3 of the SI. Contrary to the fully long-range corrected

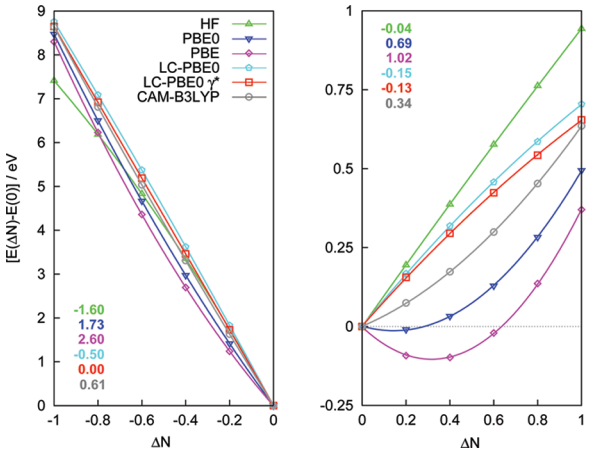

Figure 5. Ground-state energy (eV) of β-pinene as a function of deviations of fractional occupation number ΔN, $-1 \leq \Delta N \leq 0$ (left) and $0 \leq \Delta N \leq 1$ (right), calculated as the difference between actual and overall number of electrons in the neutral molecule. The energy is given relative to the energy of the neutral molecule ($\Delta N = 0$). Calculations were performed with the aug-cc-pVDZ basis set. The numerical values provide quantitative measures of curvature obtained from fitting quadratic functions to the data sets. For a single plot covering the full range $-1 \leq \Delta N \leq 1$ see Figure S5 of the SI.

functionals, no minimum is seen in Figure 4 even for a large range of γ values. Thus, the numerical data obtained for our examples support the qualitative arguments put forward in the previous paragraph, namely, that a functional that cannot establish $V_{XC}(\infty) = 0$ may not be "tunable" in the sense of eq 3.

For further tests with CAM-B3LYP, we have adopted the tuned γ^* for the LC-B3LYP functional. The MRs for CAM-B3LYP obtained with $\gamma = 0.33$ and with the γ^* are collected in Table 2. The smaller γ^* leads in most cases to worse agreement with CCSD optical rotations. The increase in relative deviations is the lowest for methyloxirane (by 1.3 to 9.7%), followed by norbornenone (13 to 28%) and β-pinene (by 68 to 1146%). For norbornenone, the CAM-B3LYP molar rotations are noticeably larger in magnitude as compared to LC-B3LYP. Accordingly, higher deviations from the CCSD and CC2 reference data are obtained. These results are in line with the increase of optical rotation magnitude when going from a fully long-range corrected LC-B3LYP of 100% to the standard global hybrid B3LYP with 20% exact exchange. The partially long-range corrected CAM-B3LYP (65% of HF exchange asymptotically) gives optical rotations between those calculated with LC-B3LYP and B3LYP. As far as β-pinene is concerned, the CAM-B3LYP parametrizations lead to MRs in least agreement with CCSD and fail to reproduce the sign at 633 nm. For all three wavelengths, a significant overestimation of the MRs can be observed. We note in passing that the original parametrization of CAM-B3LYP performs somewhat similar to the LC version with γ^*.

3.3. Calculations with Fractional Electron Numbers. The straight-line behavior of $E(N)$ was mentioned briefly in the Introduction. In this last section, we examine this behavior for β-pinene. Figure 5 shows calculated energies as a function of N around the electron number for the neutral molecule. With all density functionals as well as HF, the electron affinity is calculated to be negative. Correspondingly, the LUMO energy in the HF calculation is positive, indicating that the system will not bind an additional electron. The resulting derivative discontinuity in the $E(N)$ plot is large around $\Delta N = 0$, where the

slope changes formally from −IP to −EA. A minor negative curvature in the excess electron section ($\Delta N > 0$) of the plot is seen for the standard parametrization of LC-PBE0, but overall a nearly optimal straight line behavior is obtained. The "tuned" version is slightly better but still displays some residual negative curvature in the electron-rich part of the plot ($\Delta N > 0$). The similarity between $E(N)$ obtained with the two parametrizations is surprising at first sight, given a significant change from the default $\gamma = 0.30$ to $\gamma^* = 0.20$ to satisfy eq 3. However, this is likely a consequence of the criterion adopted here, which predominantly affects the electron deficient side of the plot and, for the tuned version of LC-PBE0, indeed leads to a vanishing curvature for $\Delta N < 0$. Interestingly, for β-pinene, HF theory gives an essentially perfect straight line for $\Delta N > 0$ (much unlike the carbon atom, see the Figure S4 of the SI), albeit with a larger slope than LC-PBE0. Other functionals considered here yield a more (PBE, PBE0) or less (CAM-B3LYP) pronounced positive curvature for $E(N)$ which is typical of functionals with delocalization errors, as discussed in refs 17 and 116.

4. CONCLUSIONS

The success or failure of system-specific adjustments of the parameters in range-separated density functionals to satisfy eq 3 or, alternatively, the straight line theorem, is perhaps best judged by the principle *primum non nocere* ("first, do no harm"). This work has examined the consequences of selecting system-specific range-separation parameters in the context of calculating optical rotations for selected difficult cases. Optical rotation (OR) is a molecular mixed electric−magnetic dynamic linear response property that is known to be sensitive to approximations made in the electronic structure model. For small molecules, comparisons were made with available coupled-cluster data (CC2, CCSD, CC3). For the interesting helicene systems, reliable CC level calculations have unfortunately not yet been reported. The performance of the functionals for helicenes and helicene derivatives must be assessed with the help of experimental data under the assumption that for these systems solution-phase effects are minor.

For β-pinene and the helicenes, the system-specific adjustment of γ tends to produce improved ORs. For the helicenes, the optimized γ of 0.14 is significantly below commonly used values (typically on the order of 0.3) which can be attributed to the extended delocalized π systems. For norbornenone, the exchange component of the functional has a drastic influence on the calculated ORs. Our results obtained with LC functionals agree reasonably well with CC2 reference data, but they are too high in magnitude when compared to available CCSD optical rotations. For methyloxirane, adjusting γ does not lead to systematic improvements, but it also appears to do no particular damage. On the basis of this initial study, one may cautiously recommend the use of system-specific range-separation parameters for response calculations in the sense that it might either improve calculated ORs while at the same time ensuring some fundamental DFT requirements, or at least not do much harm. It remains to be seen if catastrophic failures upon γ tuning will be encountered. High values of γ appear to improve calculated ORs in selected cases, but such magnitudes of γ are difficult to justify on the basis of eq 3. It is worth emphasizing at this point that the tuning procedure in its original, simplest form as proposed by Livshits and Baer in ref 37 was applied herein. Modifications have been recently proposed[46−48] in which, for example, eq 3 is employed for both the neutral and the negatively charged system and an average or root-mean-square of the two criteria is minimized. The results for the tuned LC-PBE0 functional shown in Figure 5 suggest that it might be worthwhile to consider such a criterion in future studies of OR with range-separated hybrid functionals.

■ ASSOCIATED CONTENT

Supporting Information. Tuning γ for norbornenone at the LC-BLYP and for the DFT-D3 structure of [7]helicene at the LC-PBE0 level. Tuning γ at the CAM-B3LYP level. The corresponding numerical values of $\Delta E(\gamma)$. Total energy of the C atom as a function of the electron number. Total energy of the β-pinene molecule as a function of the electron number. This material is available free of charge via the Internet at http://pubs.acs.org.

■ AUTHOR INFORMATION

Corresponding Author

*E-mail: jochena@buffalo.edu.

Notes

The authors declare no competing financial interest.

■ ACKNOWLEDGMENT

This work has been supported by grant no. CHE 0952253 from the National Science Foundation. M.S. is grateful for financial support from the Foundation for Polish Science ("START" scholarship). The authors would like to acknowledge the Center for Computational Research (CCR) at the University at Buffalo for providing computational resources. The authors thank Dr. Niranjan Govind for technical advice and helpful discussions and Prof. Jeanne Crassous for information regarding the OR of 2-alkynyl[6]helicene.

■ REFERENCES

(1) Parr, R. G.; Yang, W. *Density-Functional Theory of Atoms and Molecules*; Oxford University Press: New York, 1989.

(2) Dreizler, R. M.; Gross, E. K. U. *Density Functional Theory. An Approach to the Quantum Many-Body Problem*; Springer-Verlag: New York, 1990.

(3) Gross, E. K. U.; Dobson, J. F.; Petersilka, M. *Top. Curr. Chem.* **1996**, *181*, 81–172.

(4) Engel, E.; Dreizler, R. M. *Density Functional Theory. An Advanced Course*; Springer-Verlag: Berlin, 2011.

(5) Ziegler, T. *Chem. Rev.* **1991**, *91*, 651–667.

(6) Seminario, J. M.; Politzer, P. *Modern Density Functional Theory. A Tool for Chemistry*; Elsevier: Amsterdam, 1995.

(7) Seminario, J. M. *Recent Developments and Applications of Modern Density Functional Theory*; Elsevier: Amsterdam, 1996.

(8) Siegbahn, P. E. M.; Blomberg, M. R. A. *Annu. Rev. Phys. Chem.* **1999**, *50*, 221–249.

(9) van Doren, V.; van Alsenoy, C.; Geerlings, P. *Density Functional Theory and its Application to Materials: Antwerp, Belgium, June 8−10, 2000*; American Institute of Physics: Melville, NY, 2001.

(10) Koch, W.; Holthausen, M. C. *A Chemist's Guide to Density-Functional Theory*; Wiley-VCH: New York, 2000.

(11) Furche, F.; Ahlrichs, R. *J. Chem. Phys.* **2002**, *117*, 7433–7447.

(12) Marques, M. A. L.; Ullrich, C. A.; Nogueira, F.; Rubio, A.; Burke, K.; Gross, E. K. U. *Time-Dependent Density Functional Theory*; Springer-Verlag: Berlin, 2006.

(13) Autschbach, J. Spectroscopic Properties Obtained from Time-Dependent Density Functional Theory (TD-DFT). In *Encyclopedia of Inorganic Chemistry*; Wiley-VCH: New York, 2009. DOI: 10.1002/0470862106.ia600.
(14) Cramer, C. J.; Truhlar, D. G. *Phys. Chem. Chem. Phys.* **2009**, *11*, 10757–10816.
(15) Elliott, P.; Furche, F.; Burke, K. Excited States from Time-Dependent Density Functional Theory. In *Reviews in Computational Chemistry*; Lipkowitz, K. B., Cundari, T. R., Eds.; John Wiley & Sons, Inc.: Hoboken, NY, 2009; Vol. 26, DOI: 10.1002/9780470399545.ch3.
(16) Autschbach, J.; Nitsch-Velasquez, L.; Rudolph, M. *Top. Curr. Chem.* **2011**, *298*, 1–98.
(17) Cohen, A. J.; Mori-Sanchés, P.; Yang, W. *Science* **2008**, *321*, 792–794.
(18) Zhang, Y.; Yang, W. *J. Chem. Phys.* **1998**, *109*, 2604–2608.
(19) Champagne, B.; Perpéte, E. A.; van Gisbergen, S. J. A.; Baerends, E.; Snijders, J. G.; Soubra-Ghaoui, C.; Robins, K. A.; Kirtman, B. *J. Chem. Phys.* **1998**, *109*, 10489–10498.
(20) Dreuw, A.; Weisman, J. L.; Head-Gordon, M. *J. Chem. Phys.* **2003**, *119*, 2943–2946.
(21) Tozer, D. J. *J. Chem. Phys.* **2003**, *119*, 12697–12699.
(22) Peach, M. J. G.; Benfield, P.; Helgaker, T.; Tozer, D. J. *J. Chem. Phys.* **2008**, *128*, 044118.
(23) Autschbach, J. *ChemPhysChem* **2009**, *10*, 1–5.
(24) Perdew, J. P.; Zunger, A. *Phys. Rev. B* **1981**, *23*, 5048–5079.
(25) van Leeuwen, R.; Baerends, E. J. *Phys. Rev. A* **1994**, *49*, 2421–2431.
(26) Ullrich, C. A.; Gossmann, U. J.; Gross, E. K. U. *Phys. Rev. Lett.* **1995**, *74*, 872–875.
(27) Tozer, D. J.; Handy, N. C. *J. Chem. Phys.* **1998**, *109*, 10180–10189.
(28) Iikura, H.; Tsuneda, T.; Yanai, T.; Hirao, K. *J. Chem. Phys.* **2001**, *115*, 3540–3544.
(29) Tawada, Y.; Tsuneda, T.; Yanagisawa, S.; Yanai, T.; Hirao, K. *J. Chem. Phys.* **2004**, *120*, 8425–8433.
(30) Yanai, T.; Tew, D. P.; Handy, N. C. *Chem. Phys. Lett.* **2004**, *393*, 51–57.
(31) Baer, R.; Neuhauser, D. *Phys. Rev. Lett.* **2005**, *94*, 043002(1)–043002(4).
(32) Gerber, I. C.; Ángyán, J. G. *Chem. Phys. Lett.* **2005**, *415*, 100–105.
(33) Vydrov, O. A.; Scuseria, G. E. *J. Chem. Phys.* **2006**, *125*, 234109(1)–234109(9).
(34) Vydrov, O. A.; Heyd, J.; Krukau, A. V.; Scuseria, G. E. *J. Chem. Phys.* **2006**, *125*, 074106(1)–074106(9).
(35) Peach, M. J. G.; Helgaker, T.; Sałek, P.; Keal, T. W.; Lutnæs, O. B.; Tozer, D. J.; Handy, N. C. *Phys. Chem. Chem. Phys.* **2006**, *8*, 558–562.
(36) Vydrov, O. A.; Scuseria, G. E.; Perdew, J. P. *J. Chem. Phys.* **2007**, *126*, 154109(1)–154109(9).
(37) Livshits, E.; Baer, R. *Phys. Chem. Chem. Phys.* **2007**, *9*, 2932–2941.
(38) Chai, J.; Head-Gordon, M. *J. Chem. Phys.* **2008**, *128*, 084106(1)–084106(15).
(39) Jimènez-Hoyos, C. A.; Janesko, B. G.; Scuseria, G. E. *J. Phys. Chem. A* **2009**, *113*, 11742–11749.
(40) Steinmann, S. N.; Wodrich, M. D.; Corminboeuf, C. *Theor. Chem. Acc.* **2010**, *127*, 429–442.
(41) Peach, M. J. G.; Cohen, A. J.; Tozer, D. J. *Phys. Chem. Chem. Phys.* **2006**, *8*, 4543–4549.
(42) Lange, A. W.; Rohrdanz, M. A.; Herbert, J. M. *J. Phys. Chem. B* **2008**, *112*, 6304–6308.
(43) Rohrdanz, M. A.; Herbert, J. M. *J. Chem. Phys.* **2008**, *129*, 034107(1)–034107(9).
(44) Shcherbin, D.; Ruud, K. *Chem. Phys.* **2008**, *349*, 234–243.
(45) Song, J.; Hirosawa, T.; Tsuneda, T.; Hirao, K. *J. Chem. Phys.* **2007**, *126*, 154105(1)–154105(7).
(46) Stein, T.; Kronik, L.; Baer, R. *J. Am. Chem. Soc.* **2009**, *131*, 2818–2820.
(47) Stein, T.; Eisenberg, H.; Kronik, L.; Baer, R. *Phys. Rev. Lett.* **2010**, *105*, 266802(1)–266802(4).
(48) Kuritz, N.; Stein, T.; Baer, R.; Kronik, L. *J. Chem. Theory Comput.* **2011**, *7*, 2408–2415.
(49) Baer, R.; Livshits, E.; Salzner, U. *Annu. Rev. Phys. Chem.* **2010**, *61*, 85–109.
(50) Livshits, E.; Baer, R. *J. Phys. Chem. A* **2008**, *112*, 12789–12791.
(51) Salzner, U.; Baer, R. *J. Chem. Phys.* **2009**, *131*, 231101(1)–231101(5).
(52) Stein, T.; Kronik, L.; Baer, R. *J. Chem. Phys.* **2009**, *131*, 244119(1)–244119(5).
(53) Cohen, A. J.; Mori-Sánchez, P.; Yang, W. *J. Chem. Phys.* **2007**, *126*, 191109(1)–191109(5).
(54) Perdew, J. P.; Parr, R. G.; Levy, M.; Balduz, J. L. *Phys. Rev. Lett.* **1982**, *49*, 1691–1694.
(55) Tsuneda, T.; Song, J.; Suzuki, S.; Hirao, K. *J. Chem. Phys.* **2010**, *133*, 174101(1)–174101(9).
(56) Polavarapu, P. L.; Chakraborty, D. K. *J. Am. Chem. Soc.* **1998**, *120*, 6160–6164.
(57) Stephens, P. J.; Devlin, F. J.; Cheeseman, J. R.; Frisch, M. J.; Rosini, C. *Org. Lett.* **2002**, *4*, 4595–4598.
(58) McCann, D. M.; Stephens, P. J.; Cheeseman, J. R. *J. Org. Chem.* **2004**, *69*, 8709–8717.
(59) Giorgio, E.; Viglione, R. G.; Zanasi, R.; Rosini, C. *J. Am. Chem. Soc.* **2004**, *126*, 12968–12976.
(60) Stephens, P. J.; McCann, D. M.; Cheeseman, J. R.; Frisch, M. J. *Chirality* **2005**, *17*, S52–S64.
(61) McCann, D. M.; Stephens, P. J. *J. Org. Chem.* **2006**, *71*, 6074–6098.
(62) Autschbach, J.; Jensen, L.; Schatz, G. C.; Tse, Y. C. E.; Krykunov, M. *J. Phys. Chem. A* **2006**, *110*, 2461–2473.
(63) Stephens, P. J.; Devlin, F. J.; Cheeseman, J. R.; Frisch, M. J. *J. Phys. Chem. A* **2001**, *105*, 5356–5371.
(64) Stephens, P. J.; Devlin, F. J.; Cheeseman, J. R.; Frisch, M. J.; Bortolini, O.; Besse, P. *Chirality* **2003**, *15*, S57–S64.
(65) Crawford, T. D.; Stephens, P. J. *J. Phys. Chem. A* **2008**, *112*, 1339–1345.
(66) Srebro, M.; Govind, N.; de Jong, W. A.; Autschbach, J. *J. Phys. Chem. A* **2011**, *115*, 10930–10949.
(67) Richard, R. M.; Herbert, J. M. *J. Chem. Theory Comput.* **2011**, *7*, 1296–1306.
(68) Bylaska, E. J.; de Jong, W. A.; Govind, N.; Kowalski, K.; Straatsma, T. P.; Valiev, M.; van Dam, J. J.; Wang, D.; Apra, E.; Windus, T. L.; Hammond, J.; Autschbach, J.; Aquino, F.; Nichols, P.; Hirata, S.; Hackler, M. T.; Zhao, Y.; Fan, P.-D.; Harrison, R. J.; Dupuis, M.; Smith, D. M. A.; Glaesemann, K.; Nieplocha, J.; Tipparaju, V.; Krishnan, M.; Vazquez-Mayagoitia, A.; Jensen, L.; Swart, M.; Wu, Q.; Van Voorhis, T.; Auer, A. A.; Nooijen, M.; Crosby, L. D.; Brown, E.; Cisneros, G.; Fann, G. I.; Fruchtl, H.; Garza, J.; Hirao, K.; Kendall, R.; Nichols, J. A.; Tsemekhman, K.; Wolinski, K.; Anchell, J.; Bernholdt, D.; Borowski, P.; Clark, T.; Clerc, D.; Dachsel, H.; Deegan, M.; Dyall, K.; Elwood, D.; Glendening, E.; Gutowski, M.; Hess, A.; Jaffe, J.; Johnson, B.; Ju, J.; Kobayashi, R.; Kutteh, R.; Lin, Z.; Littlefield, R.; Long, X.; Meng, B.; Nakajima, T.; Niu, S.; Pollack, L.; Rosing, M.; Sandrone, G.; Stave, M.; Taylor, H.; Thomas, G.; van Lenthe, J.; Wong, A.; Zhang, Z. *NWChem, A Computational Chemistry Package for Parallel Computers*, version 6 (2011 developer's version); Pacific Northwest National Laboratory: Richland, WA, 2011.
(69) Valiev, M.; Bylaska, E. J.; Govind, N.; Kowalski, K.; Straatsma, T. P.; van Dam, H. J. J.; Wang, D.; Nieplocha, J.; Apra, E.; Windus, T. L.; de Jong, W. A. *Comput. Phys. Commun.* **2010**, *181*, 1477–1489.
(70) Dunning, T. H. *J. Chem. Phys.* **1989**, *90*, 1007–1023.
(71) Kendall, R. A.; Dunning, T. H.; Harrison, R. J. *J. Chem. Phys.* **1992**, *96*, 6796–6806.
(72) Perdew, J. P.; Burke, K.; Ernzerhof, M. *Phys. Rev. Lett.* **1996**, *77*, 3865–3868.

(73) Perdew, J. P.; Burke, K.; Ernzerhof, M. *Phys. Rev. Lett.* **1997**, *78*, 1396.
(74) Adamo, C.; Barone, V. *J. Chem. Phys.* **1999**, *110*, 6158–6170.
(75) Ernzerhof, M.; Scuseria, G. E. *J. Chem. Phys.* **1999**, *110*, 5029–5036.
(76) Becke, A. D. *Phys. Rev. A* **1988**, *38*, 3098–3100.
(77) Lee, C.; Yang, W.; Parr, R. G. *Phys. Rev. B* **1988**, *37*, 785–789.
(78) Vosko, S. H.; Wilk, L.; Nusair, M. *Can. J. Phys.* **1980**, *58*, 1200–1211.
(79) Stephens, P. J.; Devlin, F. J.; Chabalowski, C. F.; Frisch, M. J. *J. Phys. Chem.* **1994**, *98*, 11623–11627.
(80) Autschbach, J. *Comput. Lett.* **2007**, *3*, 131–150.
(81) Autschbach, J. *ChemPhysChem* **2011**, *12*, 3224–3235.
(82) Müller, T.; Wiberg, K. B.; Vaccaro, P. H. *J. Phys. Chem. A* **2000**, *104*, 5959–5968.
(83) Müller, T.; Wiberg, K. B.; Vaccaro, P. H.; Cheeseman, J. R.; Frisch, M. J. *J. Opt. Soc. Am. B* **2002**, *19*, 125–141.
(84) Wilson, S. M.; Wiberg, K. B.; Cheeseman, J. R.; Frisch, M. J.; Vaccaro, P. H. *J. Phys. Chem. A* **2005**, *109*, 11752–11764.
(85) Mach, T. J.; Crawford, T. D. *J. Phys. Chem. A* **2011**, *115*, 10045–10051.
(86) Pedersen, T. B.; Koch, H.; Boman, L.; de Merás, A. M. J. S. *Chem. Phys. Lett.* **2004**, *393*, 319–326.
(87) Tam, M. C.; Russ, N. J.; Crawford, T. D. *J. Chem. Phys.* **2004**, *121*, 3550–3557.
(88) Kongsted, J.; Pedersen, T. B.; Strange, M.; Osted, A.; Hansen, A. E.; Mikkelsen, K. V.; Pawlowski, F.; Jørgensen, P.; Hättig, C. *Chem. Phys. Lett.* **2005**, *401*, 385–392.
(89) Kumata, Y.; Furukawa, J.; Fueno, T. *Bull. Chem. Soc. Jpn.* **1970**, *43*, 3920–3921.
(90) Lightner, D. A.; Gawronski, J. K.; Bouman, T. D. *J. Am. Chem. Soc.* **1980**, *102*, 5749–5754.
(91) Brown, H. C.; Zaidlewicz, M.; Bhat, K. S. *J. Org. Chem.* **1989**, *54*, 1764–1766.
(92) Ruud, K.; Zanasi, R. *Angew. Chem., Int. Ed.* **2005**, *44*, 3594–3596.
(93) Crawford, T. D.; Tam, M. C.; Abrams, M. L. *Mol. Phys.* **2007**, *105*, 2607–2617.
(94) Mort, B. C.; Autschbach, J. *Chem. Phys. Chem* **2008**, *9*, 159–170.
(95) Frisch, M. J.; Trucks, G. W.; Schlegel, H. B.; Scuseria, G. E.; Robb, M. A.; Cheeseman, J. R.; Scalmani, G.; Barone, V.; Mennucci, B.; Petersson, G. A.; Nakatsuji, H.; Caricato, M.; Li, X.; Hratchian, H. P.; Izmaylov, A. F.; Bloino, J.; Zheng, G.; Sonnenberg, J. L.; Hada, M.; Ehara, M.; Toyota, K.; Fukuda, R.; Hasegawa, J.; Ishida, M.; Nakajima, T.; Honda, Y.; Kitao, O.; Nakai, H.; Vreven, T.; Montgomery, J. A., Jr.; Peralta, J. E.; Ogliaro, F.; Bearpark, M.; Heyd, J. J.; Brothers, E.; Kudin, K. N.; Staroverov, V. N.; Kobayashi, R.; Normand, J.; Raghavachari, K.; Rendell, A.; Burant, J. C.; Iyengar, S. S.; Tomasi, J.; Cossi, M.; Rega, N.; Millam, J. M.; Klene, M.; Knox, J. E.; Cross, J. B.; Bakken, V.; Adamo, C.; Jaramillo, J.; Gomperts, R.; Stratmann, R. E.; Yazyev, O.; Austin, A. J.; Cammi, R.; Pomelli, C.; Ochterski, J. W.; Martin, R. L.; Morokuma, K.; Zakrzewski, V. G.; Voth, G. A.; Salvador, P.; Dannenberg, J. J.; Dapprich, S.; Daniels, A. D.; Farkas, Ö.; Foresman, J. B.; Ortiz, J. V.; Cioslowski, J.; Fox, D. J. *Gaussian 09*, Revision A.1; Gaussian, Inc.: Wallingford, CT, 2009.
(96) Woon, D. E.; Dunning, T. H. *J. Chem. Phys.* **1994**, *100*, 2975–2988.
(97) Moscowitz, A. *Adv. Chem. Phys.* **1962**, *4*, 67–112.
(98) Wiberg, K. B.; Wang, Y. G.; Wilson, S. M.; Vaccaro, P. H.; Cheeseman, J. R. *J. Phys. Chem. A* **2006**, *110*, 13995–14002.
(99) Ruud, K.; Stephens, P. J.; Devlin, F. J.; Taylor, P. R.; Cheeseman, J. R.; Frisch, M. J. *Chem. Phys. Lett.* **2003**, *373*, 606–614.
(100) Autschbach, J.; Patchkovskii, S.; Ziegler, T.; van Gisbergen, S. J. A.; Baerends, E. J. *J. Chem. Phys.* **2002**, *117*, 581–592.
(101) Krykunov, M.; Autschbach, J. *J. Chem. Phys.* **2005**, *123*, 114103–10.
(102) Mort, B. C.; Autschbach, J. *J. Phys. Chem. A* **2005**, *109*, 8617–8623.
(103) Christiansen, O.; Koch, H.; Jørgensen, P. *Chem. Phys. Lett.* **1995**, *243*, 409–418.
(104) Wong, B. M.; Hsieh, T. H. *J. Chem. Theory Comput.* **2010**, *6*, 3704–3712.
(105) Murphy, V. L.; Kahr, B. *J. Am. Chem. Soc.* **2011**, *133*, 12918–12921.
(106) Lopata, K.; Reslan, R.; Kowalska, M.; Neuhauser, D.; Govind, N.; Kowalski, K. *J. Chem. Theory Comput.* **2011**, *7*, 3686–3693.
(107) Anger, E.; Srebro, M.; Vanthuyne, N.; Toupet, L.; Roussel, C.; Autschbach, J.; Crassous, J.; Réau, R. 2011, in preparation.
(108) Martin, R. H.; Flammang-Barbieux, M.; Cosyn, J. P.; Gelbcke, M. *Tetrahedron Lett.* **1968**, *9*, 3507–3510.
(109) Newman, M. S.; Lutz, W. B.; Lednicer, D. *J. Am. Chem. Soc.* **1955**, *77*, 3420–3421.
(110) Lightner, D. A.; Hefelfinger, D. T.; Powers, T. W.; Frank, G. W.; Trueblood, K. N. *J. Am. Chem. Soc.* **1972**, *94*, 3492–3497.
(111) Grimme, S.; Antony, J.; Ehrlich, S.; Krieg, H. *J. Chem. Phys.* **2010**, *132*, 154104–154119.
(112) Grimme, S.; Mück-Lichtenfeld, C.; Antony, J. *J. Phys. Chem. C* **2007**, *111*, 11199–11207.
(113) Norel, L.; Rudolph, M.; Vanthuyne, N.; Williams, J. A. G.; Lescop, C.; Roussel, C.; Autschbach, J.; Crassous, J.; Réau, R. *Angew. Chem., Int. Ed.* **2010**, *49*, 99–102.
(114) Anger, E.; Rudolph, M.; Norel, L.; Zrig, S.; Shen, C.; Vanthuyne, N.; Toupet, L.; Williams, J. A. G.; Roussel, C.; Autschbach, J.; Crassous, J.; Réau, R. *Chem.—Eur. J.* **2011**, *17*, 14178−14198.
(115) Perdew, J. P.; Levy, M. *Phys. Rev. Lett.* **1983**, *51*, 1884–1887.
(116) Mori-Sánchez, P.; Cohen, A. J.; Yang, W. *Phys. Rev. Lett.* **2008**, *100*, 146401(1)–146401(4).